Anticancer effects and the mechanism underlying 2-methoxyestradiol in human osteosarcoma *in vitro* and *in vivo*

XIAOYAN TANG[1*], FENGHUA TAO[2*], WEI XIANG[2], YINGCHUN ZHAO[2], LIN JIN[2] and HAI TAO[2]

[1]General Department, Zhongnan Hospital of Wuhan University, Wuhan, Hubei 430071;
[2]Department of Orthopedics, Renmin Hospital of Wuhan University, Wuhan, Hubei 430060, P.R. China

Received August 8, 2019; Accepted June 22, 2020

DOI: 10.3892/ol.2020.11925

Abstract. Osteosarcoma (OS) occurs in both children and adolescents and leads to a poor prognosis. 2-methoxyestradiol (2-ME) has a strong antitumor effect and is effective against numerous types of tumor. However, 2-ME has a low level of antitumor effects in OS. The present study investigated the effects of 2-ME on the proliferation and apoptosis of human MG63 OS cells. The potential biological mechanisms by which 2-ME exerts its biological effects were also investigated in the present study. The results of the present study demonstrated that 2-ME inhibited the proliferation of OS cells in a time- and dose-dependent manner, induced G_2/M phase cell cycle arrest and early apoptosis. The expression levels of vascular endothelial growth factor (VEGF), Bcl-2 and caspase-3 were measured via western blotting and reverse transcription-quantitative PCR. As the concentration of 2-ME increased, the RNA and protein expression levels of VEGF and Bcl-2 decreased gradually, whereas the expression of caspase-3 increased gradually. In addition, tumor growth in nude mice was suppressed by 2-ME with no toxic side effects observed in the liver or kidney. Immunohistochemistry demonstrated that the expression levels of Bcl-2 and VEGF were significantly lower, and those of caspase-3 were significantly higher in test mice compared with the control group. TUNEL staining of xenograft tumors revealed that with increased 2-ME concentration, the number of apoptotic cells also gradually increased. Thus, 2-ME effectively inhibited the proliferation and induced apoptosis of MG63 OS cells *in vitro* and *in vivo* with no obvious side effects. The mechanism of the anticancer effect of 2-ME may be associated with the actions of Bcl-2, VEGF and caspase-3.

Correspondence to: Dr Hai Tao, Department of Orthopedics, Renmin Hospital of Wuhan University, 99 Zhang Zhidong Road, Wuhan, Hubei 430060, P.R. China
E-mail: taohai2004@163.com

*Contributed equally

Key words: apoptosis, 2-methoxyestradiol, osteosarcoma, proliferation

Introduction

Osteosarcoma (OS) is the most common primary malignant bone tumor in children and adolescents globally since >100 years (1). Although surgery combined with high-dose drug therapy can improve the survival rate of patients with OS, a significant number of patients develop fatal metastatic disease or a serious treatment complication (2). Over the past few decades, despite increases in the doses of chemotherapy drugs, changes in drug use times and the use of multidrug combination chemotherapies, the survival rate of patients with OS has not substantially improved (3). The use of high dose chemotherapy drugs has significantly increased side effects in patients with OS (4). The development of new and specific treatment options and the discovery of new biomarkers are therefore necessary to improve treatment strategies for patients with OS.

2-methoxyestradiol (2-ME; 17β-2-methoxy-est-1, 3, 5(10)-triene-3,17-diol) is a normal metabolite of estradiol in humans (5). 2-ME is abundant in the blood and urine of the human body, has certain selective killing effects on tumor cells and no toxic side effects on normal cells (6). Numerous studies performed using cell lines and in animals, demonstrated that 2-ME has a potent antitumor effect against a number of different types of tumor (7-10). It has also been reported that 2-ME has antitumor effects on lung cancer, angiosarcoma, prostate cancer, colon cancer, melanoma and breast cancer cells (11-16). The antitumor effect of 2-ME has been widely studied as a promising anticancer drug. 2-ME exerts a variety of biological effects such as tumor cell cycle arrest, apoptosis and inhibition of tumor angiogenesis in cell lines (6). 2-ME is highly cytotoxic to OS cells, but not cytotoxic to normal osteoblasts (17). 2-ME may therefore have potential clinical benefits in the treatment of tumors, as it inhibits the proliferation of numerous human tumor cell lines *in vitro* (18).

Caspase is a protease that promotes apoptosis and is therefore central to the mechanism of apoptosis (19). Caspase-3 is a frequently activated death protease that catalyzes the specific cleavage of a number of key cellular proteins (20). Caspase-3 is a typical marker of apoptosis and is essential for apoptosis, chromatin condensation and DNA fragmentation in all cell types (21). Caspase-3 is also considered to be the most important scorpion caspase of apoptosis and can be activated by caspase (22). Cleavage by caspase-3 results in DNA

fragmentation, degradation of the cytoskeleton and nuclear proteins, cross-linking of proteins, formation of apoptotic bodies, ligand expression of phagocytic receptors and uptake by phagocytic cells (23). Caspase-3 is therefore essential for certain processes associated with the disintegration of cells and the formation of apoptotic bodies, but it can also function before the initiation of cell loss (24).

Bcl-2 is an important apoptotic gene and regulatory protein that can inhibit apoptosis and participate in the regulation of cell proliferation (25). It plays an important role in prolonging cell life (26). Bcl-2 activation and abnormal expression is associated with the occurrence and development of tumors (27). It also plays an important role in the formation of multidrug resistance in tumors (28). Numerous studies have confirmed that the Bcl-2 gene is closely associated with the occurrence of a variety of malignant tumors (29-31). A study has reported that the Bcl-2 gene is upregulated in the process of inhibiting apoptosis, greatly increasing the probability of cell chromosomal mutation, and normal cell infection (32). This could be the key cause of tumorigenesis in normal cells. Chemotherapy drugs that inhibit Bcl-2 protein directly or indirectly against the inhibition of apoptotic proteins increase the sensitivity of chemotherapy drugs and decrease the occurrence of tumor resistance (19).

Vascularization and nutrition are essential for tumor growth and progression. VEGF is a member of the angiogenic factor family, which plays an important role in tumor angiogenesis by promoting the proliferation and migration of cancer cells (24). VEGF has been demonstrated to be one of the most important cytokines regulating angiogenesis (25). It specifically acts on vascular endothelial cells, participates in tumor angiogenesis and is closely associated with biological characteristics such as invasion and metastasis of tumors (26). Tumor growth is inseparable from sustained and extensive angiogenesis, and inhibition of neovascularization of tumors may be an effective method for treating tumors (27). As the expression of VEGF is closely associated with angiogenesis and tumor cell proliferation, inhibiting and blocking the biological activity of VEGF secreted by tumor cells is important for suppressing tumor growth and metastasis (28).

In the present study, different concentrations of 2-ME were used to treat MG63 OS cells *in vitro* and *in vivo* to determine the effects on the proliferation, apoptosis of OS cells. Side effects were also monitored and the potential mechanism of action of 2-ME and association with other proteins was investigated. The antitumor mechanism of 2-ME as a treatment for OS remains unclear and further studies are required for elucidation.

Materials and methods

Chemicals and reagents. DMEM was purchased from Invitrogen; Thermo Fisher Scientific, Inc. 2-ME was obtained from Merck KGaA. The TUNEL assay, western blotting kits, PCR kits and MTT reagent were purchased from Boster Biological Technology.

Cell lines and cell culture. The MG63 cell line was obtained from the Department of Central Laboratory, Renmin Hospital of Wuhan University. The cells were routinely cultured under 5% (v/v) CO_2 at 37˚C and 100% relative humidity; in DMEM medium containing 10% fetal bovine serum (Invitrogen; Thermo Fisher Scientific, Inc.) and supplemented with 1% penicillin-streptomycin. The incubator was periodically sterilized.

MTT assay. OS MG63 cells were seeded into 96-well culture plates at $5x10^5$ cells/ml. The tested concentrations of 2-ME were 0, 10, 20 and 40 μmol/l. There were 6 replicate wells evaluated at each concentration. Cells were cultured for 24, 36 or 48 h. A total of 20 μl of MTT (5 mg/ml) solution were added 4 h before the end of culturing and DNA methylation was evaluated after the addition of 200 μl DMSO. This was followed by shaking to dissolve the formazan crystals, with color development (A values) assessed spectrophotometrically (Sunrise; Tecan Group Ltd.) by measuring the absorbance at 590 nm using an automated microplate reader. Cell growth inhibition rates were calculated using the formula: Inhibition rate (%)=(1-experimental group A value/control group A value) x100%. All data are the averages of those from 6 independent experiments.

Flow cytometry for cell cycle analysis. OS MG63 cells were seeded into 96-well culture dishes at 10^6 cells/ml and 2-ME added to 0, 10, 20 or 40 μM (6 wells/group). After 2 days of culture, trypsin was added and the cell suspensions centrifuged (1,000 x g for 5 min at room temperature). The cells were collected and incubated with RNase A for 30 min, propidium iodide (PI) reagent (BD Biosciences) was then added and the cells incubated in the dark for a further 30 min. Finally, the cells were analyzed by flow cytometry using a FACSCanto II (BD Biosciences), and data were analyzed using Cell Quest Pro software version 5.1 (BD Biosciences).

Apoptosis assay. OS MG63 cells were seeded into 6-well plates at $3x10^5$ cells/well and cultured for 12-24 h with different concentrations of 2-ME (0, 10, 20 or 40 μM). After 24 h, the cells were digested with trypsin (without EDTA), and the individual cell suspensions were transferred to flow tubes and centrifuged at 1,000 x g for 5 min at room temperature. The supernatants were discarded, the cells washed twice, and 875 μl of apoptosis kit buffer, annexin V-fluorescein isothiocyanate (FITC), and PI solution (Beijing TransGen Biotech Co. Ltd.) added according to the manufacturer's protocol. The extent of apoptosis was measured by flow cytometry using a FACSCanto II (BD Biosciences), and data were analyzed using Cell Quest Pro software version 5.1 (BD Biosciences). Dual FITC/PI staining can accurately distinguish cells in different stages of apoptosis (33).

Western blotting. Cells in the logarithmic phase of growth were collected and resuspended in DMEM medium for 24 h at 37˚C. Subsequently, 2-ME was added to the cells at different concentrations, the cells were incubated. Total proteins were prepared using the Nuclear and Cytoplasmic Protein Extraction kit (Beyotime Institute of Biotechnology), and the concentration was determined by a BCA Protein assay kit (Bio-Rad Laboratories, Inc.). Proteins (40 μg/lane) were separated by 10% SDS-PAGE and transferred to polyvinylidene fluoride membrane (Bio-Rad Laboratories, Inc.). Cell debris collected and lysed to extract proteins. After blocking

in 5% skimmed milk for 1 h at room temperature, the solutions were incubated with primary antibodies (1:100; cat. no. 1315; Sigma-Aldrich; Merck KGaA) against Bcl-2, VEGF, caspase-3, or β-actin at 4˚C for 16 h, followed by incubation with an appropriate secondary antibody (1:10,000; cat. no. BA1055; Boster Biological Technology) conjugated to horseradish peroxidase at room temperature for 60 min and then the luminescent reagents A and B from the western blotting kit (Goodbio Technology). The signal was visualized using enhanced chemiluminescent reagent (cat. no. KGP1121; Nanjing KeyGen Biotech Co., Ltd.). The membranes were exposed to X-ray films, which were then developed. β-actin was used as the reference protein. The expression levels of target proteins were determined using densitometry (the gray intensities were derived), and Image J software version 1.0 (National Institutes of Health) was used for quantitative analysis of the bands.. The expression levels of target proteins in the control and experimental groups were statistically compared.

RNA extraction and reverse transcription-quantitative (RT-q) PCR. The PrimeScript RT Reagent kit (Boster Biological Technology, Ltd.) was used and the samples were incubated at 37˚C for 15 min followed by 85˚C for 5 sec and then maintained at 4˚C. Cells in the logarithmic phase of growth were collected, suspended in fresh medium and different concentrations of 2-ME added. After 48 h, the cells were collected and 1 ml TRIzol® reagent (Thermo Fisher Scientific, Inc.) added to obtain RNA solutions. Each RNA reaction mixture included Taq enzyme, dNTP mix, loading dye, DNA template, ddH_2O, the reverse transcription reaction product and forward and reverse primers. The following primers were used: Bcl-2 forward, 5'-CAGGAAACGGCCCGGAT-3' and reverse, 5'-CTGGGGCCTTTCATCCTCC-3'; VEGF forward, 5'-GGGAGCAGAAAGCCCATGAA-3' and reverse, 5'-AGATGTCCACCAGGGTCTCA-3'; caspase-3 forward, 5'-CTCGGTCTGGTACAGATGTCGATG-3' and reverse, 5'-GGTTAACCCGGGTAAGAATGTGCA-3'; and β-actin forward, 5'-CATTAAGGAGAAGCTGTGCT-3' and reverse, 5'-GTTGAAGGTAGTTTCGTGGA-3'. Pre-denaturation was performed for 93˚C for 3 min, followed by 36 cycles of 95˚C for 5 min, 93˚C for 40 sec and 72˚C for 60 sec. β-actin was used as the internal reference gene. Amplification curves were drawn and the relative mRNA expression levels were calculated using $2^{-\Delta\Delta Cq}$ (34).

Tumor xenograft growth in nude mice. BALB/c nude mice (n=32) were purchased from the Center of Wuhan University; all were male, 4 weeks of age and weighed 18-24 g, which was the weight at the start of the study. The animals were raised in specific pathogen free-class sterile individually ventilated cages. The experimental animal program was approved by the Experimental Animal Care Committee (approval no. S01315022I) of Renmin Hospital, Wuhan University (Wuhan, China). OS MG63 cells (0.1 ml, $1x10^7$) in the logarithmic growth phase were subcutaneously injected into the right hips of the nude mice. After 1 week, when all mice had developed subcutaneous masses, they were randomly divided into 4 groups that received 2-ME at 0, 10, 20 or 40 mg/kg/day for 30 consecutive days. During drug administration, the longest diameters (a) and the shortest diameters (b) of all tumors were measured every 5 days. Tumor volume was calculated as $V=ab^2/2$ mm^3 and volume curves were drawn. After 30 days of drug administration, blood was collected from the eyeballs of mice under anesthesia, and assayed for the serum levels of alanine aminotransferase (ALT), aspartate aminotransferase (AST), creatinine (Cr) and blood urea nitrogen (BUN) to evaluate the effects of 2-ME on liver and kidney function. The mice were then sacrificed by cervical dislocation, and the subcutaneous tumors isolated and weighed. The main humane end-point used in the present study was that the tumor burden should not exceed 10% of the animal's normal body weight.

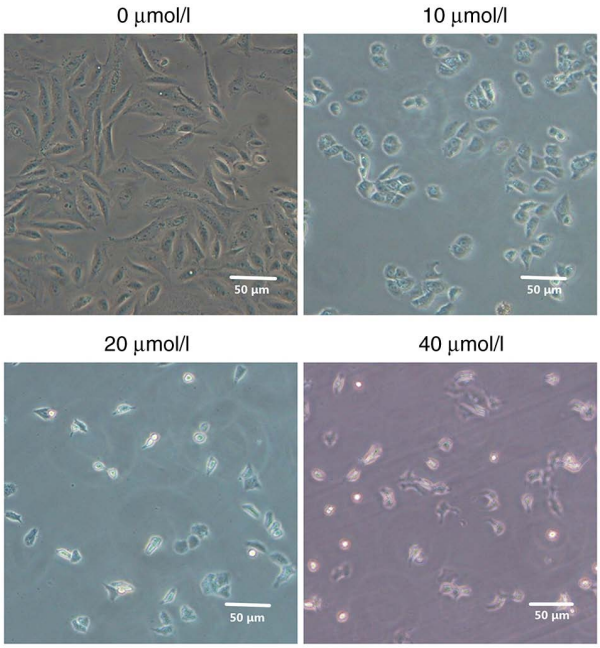

Figure 1. Morphological changes in MG63 cells (as observed under an inverted microscope) after exposure of cells to different concentrations of 2-ME for 24 h.

Immunohistochemical staining. Isolated tumor tissues were fixed in 10% formaldehyde at 4˚C for 24 h, soaked in 100% alcohol for 5 min, rendered transparent with xylene, embedded in paraffin and sectioned into 4-μm sections. Staining was performed by dropping hematoxylin and eosin solutions for 15 min at room temperature on sections placed under an inverted microscope. The sections were air-dried, soaked in xylene and peroxidase and then 10% FBS (Wuhan Servicebio Technology Co., Ltd.) was added dropwise at 37˚C for 30 min. Rabbit anti-human primary antibody (1:500; cat. no. 250713; R&D Systems, Inc.) was added and the slides placed in the refrigerator at 4˚C overnight. Following which rabbit anti-human secondary antibody (1:1,000; cat. no. sc69786; Santa Cruz Biotechnology, Inc.) VEGF, Bcl-2 and caspase-3 conjugated to horseradish peroxidase was added at 37˚C for 20 min. The sections were counterstained with hematoxylin, air-dried, and placed in xylene to render the tissues transparent for 5 min at 37˚C. Immunohistochemical staining was observed under the light microscope (IX71; Olympus Corporation; magnification, x200).

TUNEL staining. In order to detect tumor apoptosis, TUNEL staining was performed using a TUNEL assay kit according to the manufacturer's instructions. Following treatment with drugs (TMZ, 300 μM; BKM120, 300 nM) for 24 h and washing

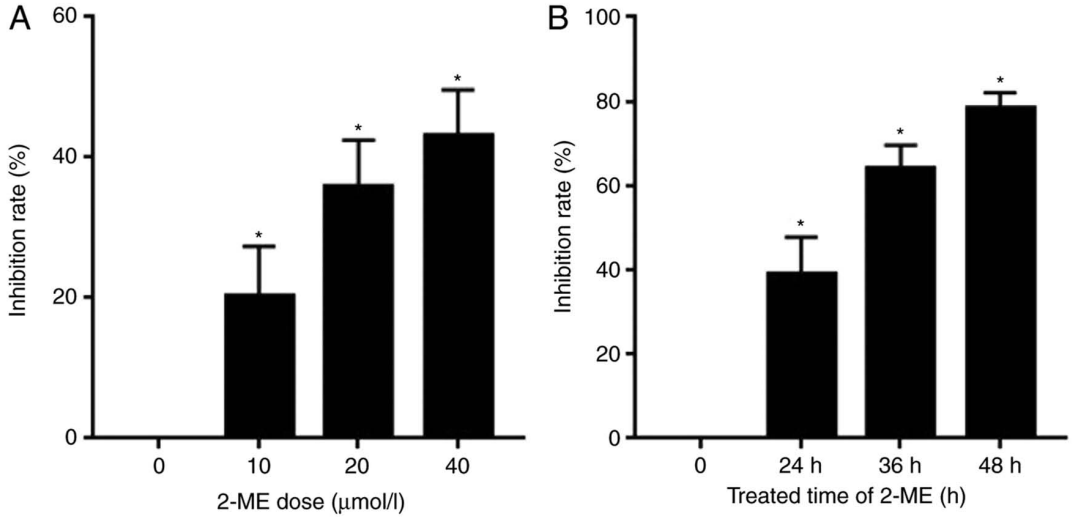

Figure 2. Effect of 2-ME on osteosarcoma cell proliferation. MG63 cells were cultured and subsequently incubated with the indicated concentrations of 2-ME for 24, 36 or 48 h and cell proliferation was measured (n=3). The results are expressed as percentages of the control and the data were analyzed using Student's unpaired t-tests. *P<0.05 compared to negative control, 2-ME, 2-methoxyestradiol.

with PBS 3 times, the cells were incubated with stationary liquid (4% paraformaldehyde) for 30 min at room temperature. The sections were air-dried, soaked in xylene and peroxidase solution added dropwise. The TUNEL reaction mixture was also added drop-wise at 37˚C for 1 h. After air drying, the converter-POD reaction solution was added drop-wise, followed by the 0.05% DAB reaction substrate (drop wise) for 1 h at room temperature. After hematoxylin staining, the slides were placed in xylene to render the tissues transparent and the slides were then sealed with a neutral gum and evaluated under a fluorescence microscope (magnification, x100). The nuclei of apoptotic cells stained brown; such cells were counted in 5 random fields and apoptosis rates calculated.

Statistical analysis. All data are presented as the mean ± SD. All statistical analyses were performed using SPSS statistical software for Windows (version 20.0; IBM Corp). All experiments were repeated at least 3 times. One-way ANOVA followed by the Tukey's test and unpaired t-tests were used to evaluate the significance of the differences between the groups. P<0.05 was considered to indicate a statistically significant difference.

Results

Morphological observations. Following treatment of MG63 cells with different concentrations of 2-ME, the effects on cell morphology were evaluated. Compared with the control group, MG63 cells exhibited morphological changes that increased significantly as the 2-ME concentration increased. Also, the cell density was significantly decreased and the cells became gradually rounded and shrunken in a 2-ME dose-dependent manner (Fig. 1).

2-ME inhibits OS cell proliferation in a dose- and time-dependent manner. The effects of 2-ME on OS cell proliferation were investigated using the MTT assay. Following 24 h of different doses of 2-ME exposure, cell proliferation was inhibited in a dose-dependent manner (Fig. 2A). After 24, 36 or 48 h of drug exposure, 2-ME was observed to inhibit cell proliferation in a time-dependent manner (Fig. 2B).

2-ME exposure causes cell cycle arrest and increased apoptosis of MG63 cells. In order to further evaluate the effect of 2-ME treatment on cell proliferation, flow cytometry was performed. The results demonstrated that 2-ME affected the MG63 cell cycle. The majority of the cells were arrested in the G_0/G_1 phase of the cell cycle, proportions of cells in S and G_2/M phases of the cell cycle were decreased (Fig. 3A). Taken together, these results demonstrated that 2-ME inhibits cell proliferation.

The effect of 2-ME on apoptosis in MG63 cells was investigated using Annexin V-FITC/PI double staining followed by flow cytometry. MG63 cells were exposed to 0, 10, 20 or 40 μM 2-ME for 24 h and the apoptosis rate was measured. The early and late apoptosis rates compared to the control gradually increased as concentration of 2-ME increased from 10 to 40 μM and were significant (P<0.05; Fig. 3B). The flow cytometry results demonstrated that 2-ME induced apoptosis in MG63 OS cells in a dose-dependent manner (Fig. 3B).

2-ME has a dose-dependent effect on the expression levels of VEGF, Bcl-2 and caspase-3. In order to elucidate the biological mechanisms involved in the proliferation and apoptotic effects of 2-ME, the expression levels of VEGF, Bcl-2 and caspase-3 were measured. MG63 cells were exposed to different doses of 2-ME for 24 h, and VEGF, Bcl-2 and caspase-3 expression levels were assessed via RT-qPCR and western blotting. The mRNA expression levels of Bcl-2 (Fig. 4B) and VEGF (Fig. 4C) in MG63 osteosarcoma cells decreased gradually with increasing 2-ME doses, whereas the expression of caspase-3 (Fig. 4D) increased gradually; the protein expression levels of Bcl-2 and VEGF in MG63 osteosarcoma cells decreased gradually with increasing 2-ME doses, whereas the expression of caspase-3 increased gradually (Fig. 4A), suggesting a dose-dependent association between Bcl-2, VEGF, caspase-3 and 2-ME (Fig. 4).

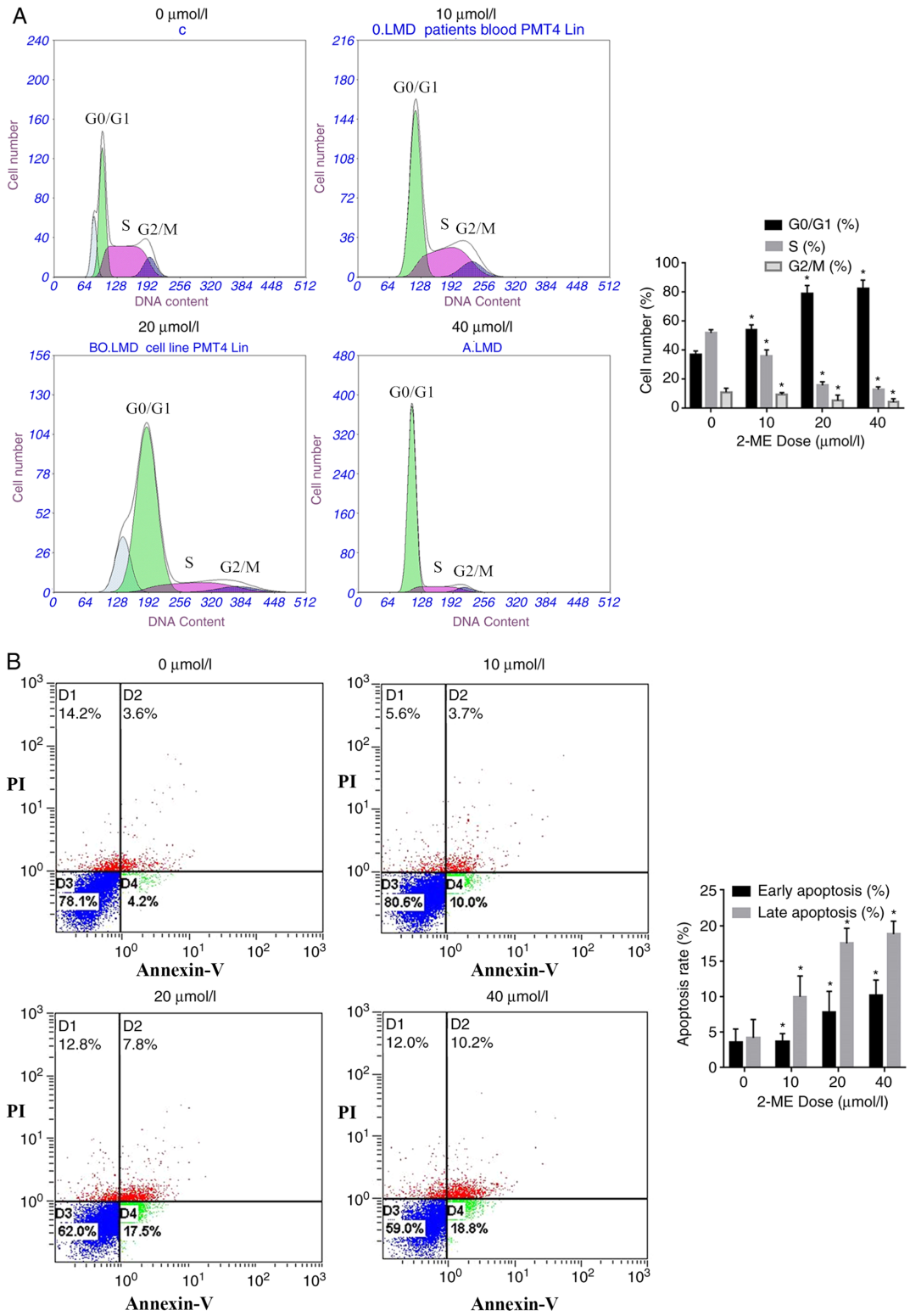

Figure 3. Effect of 2-ME on MG63 cell cycle arrest and apoptosis. (A) Flow cytometry histograms of cell number vs. DNA content to investigate cell cycle arrest. Quantification of cell number is also presented. (B) Flow cytometry plots with quantitative data displaying apoptosis of MG63 cells exposed to different concentrations of 2-ME for 24 h. *P<0.05. 2-ME, 2-methoxyestradiol.

2-ME decreases tumor development in vivo. MG63 cells were used to establish xenograft models *in vivo* and the antitumor activity of 2-ME was evaluated. Tumor volume was recorded every 5 days during the drug administration period (Fig. 5A). All experimental groups representing the different administered doses of 2-ME exhibited slower growth of transplanted tumors compared with the control group (Fig. 5A). As the 2-ME concentration increased, the inhibitory effect became more potent (Fig. 5A). After 30 days of drug administration, the mice were sacrificed and the tumor tissues removed and weighed. The diameter of the largest tumor was 1.02 cm at the end of the experiment. The tumor weights of all experimental

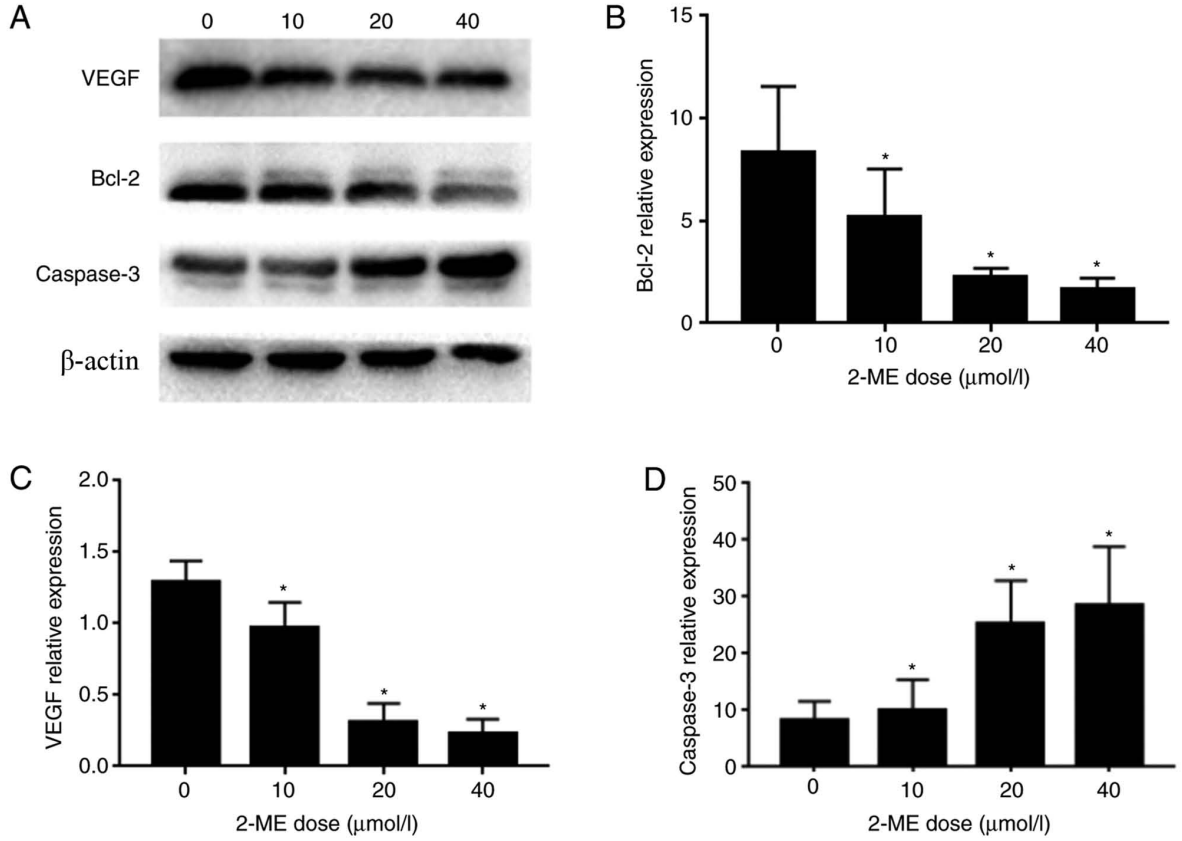

Figure 4. Effect of 2-ME on the expression levels of VEGF, Bcl-2 and caspase-3. (A) MG63 cells were treated with 0, 10, 20 or 40 μM of 2-ME for 24 h, followed by western blotting using the appropriate antibodies. β-actin was used as the control. (B-D) Bcl-2, VEGF, and caspase-3 mRNA levels normalized to β-actin mRNA levels. The data are expressed as the mean ± SD (n=3). *P<0.05. 2-ME, 2-methoxyestradiol; VEGF, vascular endothelial growth factor; SD, standard deviation.

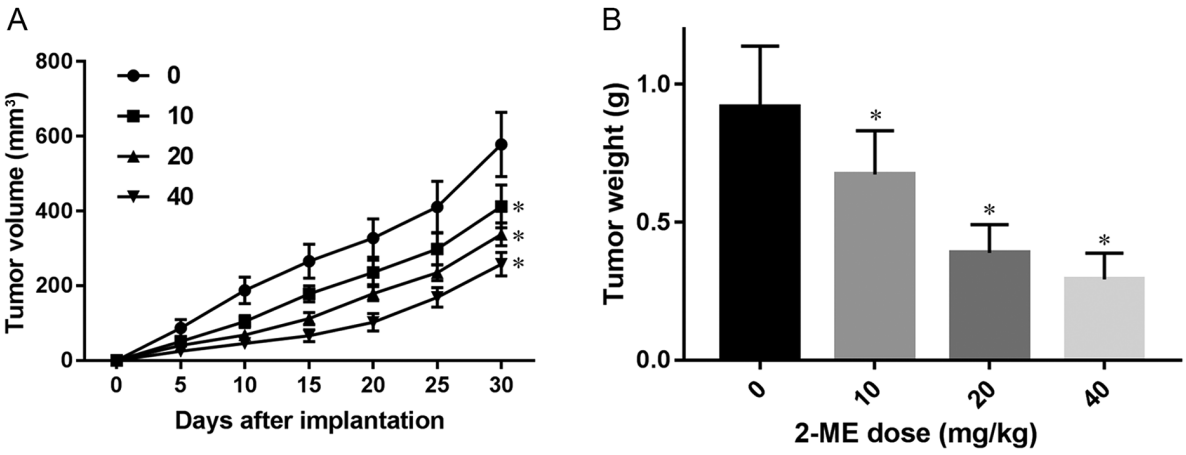

Figure 5. Effects of 2-ME on MG63 xenograft in BALB/c nude mice (n=32). (A) Tumor volume and (B) weight after implantation. *P<0.05. 2-ME, 2-methoxyestradiol.

groups were lower compared with the control group. As the 2-ME concentration increased, tumor weight increased at a slower rate in a dose-dependent manner (Fig. 5B).

Pathological features of xenograft tumors. H&E staining of xenograft tumors revealed that compared with the control group, the experimental groups demonstrated different degrees of tumor cell density reduction, scattered tissue structure (Fig. 6A) In addition, some cells exhibited nuclear pyknosis and nuclear lysis, particularly in the group treated with 40 mg/kg of 2-ME, which demonstrated liquefaction necrosis in the center of the tumor (Fig. 6A).

In order to investigate the expression levels of VEGF, Bcl-2 and caspase-3 *in vivo*, immunohistochemical staining of xenograft tumors was performed. The expression levels of Bcl-2 and VEGF in tumor tissues were decreased incrementally with increasing 2-ME concentrations, whereas the expression levels of caspase-3 gradually increased (Fig. 6B).

Table I. Effect of 2-ME on mouse liver and kidney function.

2-ME, mg/kg	No. of mice, n	ALT, μ/l	AST, μ/l	BUN, μmol/l	Cr, μmol/l
0	8	24.60±2.98	107.75±13.46	4.82±0.52	18.39±4.08
10	8	24.43±2.18	109.07±14.75	5.49±0.69	20.25±4.57
20	8	24.74±3.43	102.18±16.76	4.04±0.83	19.43±5.45
30	8	25.19±2.57	111.59±19.51	5.35±0.44	21.95±4.42

Data are presented as the mean ± standard deviation. The groups of nude BALB/c mice were treated as follows: 10 mg/kg/day saline; 10 mg/kg/day 2-ME; 20 mg/kg/day 2-ME or 40 mg/kg/day 2-ME. None of the AST, ALT, Cr or BUN levels differed significantly among the groups. ALT, alanine aminotransferase; AST, aspartate aminotransferase; Cr, creatinine; BUN, blood urea nitrogen.

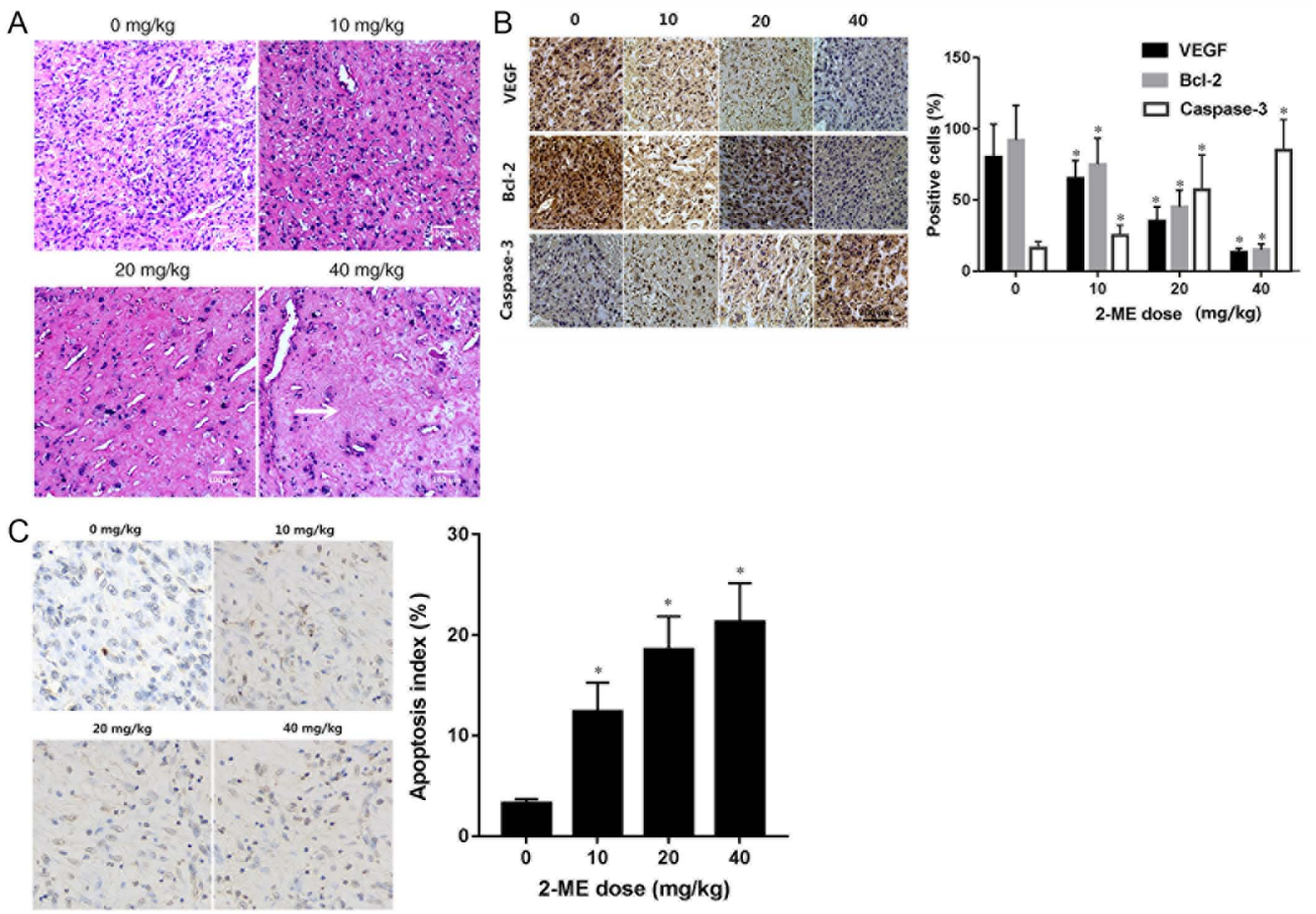

Figure 6. Immunohistochemistry and TUNEL staining of xenograft tumors. (A) Hematoxylin and eosin staining of xenograft tumors. (B) Immunohistochemistry with specific antibody against VEGF, Bcl-2, and caspase-3 in xenograft tumors. (C) TUNEL staining of apoptotic xenograft tumor cells in the 4 groups. Quantitative result of TUNEL assay is displayed. There are a few positive cells (brown staining) in the control group. *P<0.05. 2-ME, 2-methoxyestradiol; VEGF, vascular endothelial growth factor.

To confirm apoptosis in xenograft tumors, TUNEL staining was used to demonstrate that the number of apoptotic cells in the treatment groups were significantly higher than in the control group. The results also demonstrated that with increasing 2-ME concentrations, the number of apoptotic cells and the degree of apoptosis gradually increased (Fig. 6C).

2-ME treatment has no liver and kidney side effects in vivo. In order to investigate the effects of 2-ME on the liver and kidney functions of OS-bearing nude mice, the serum ALT, AST, Cr and BUN values were measured. There were no significant differences between the experimental groups and the control group (all P>0.05; Table I). Thus, 2-ME did not impair the liver or kidney functions of nude mice.

Discussion

2-ME inhibits the proliferation of animal and human tumor cells (35). It is generally considered that the mechanism of action of 2-ME against cell proliferation is primarily associ-

ated with inhibition of microtubule function and disruption of normal microtubule function and stability (36). In the present study, human OS cell proliferation was inhibited in a dose-dependent manner following 2-ME treatment, indicating that 2-ME blocks cell proliferation and induces cell cycle arrest and apoptosis.

In the present study, cell morphology investigations revealed that with increased concentrations of 2-ME, the number of OS MG63 cells gradually decreased, and the cell density significantly decreased. Cells gradually shrunk and became rounded. Furthermore, the MTT assay demonstrated that 2-ME inhibited the proliferation of MG63 cells in a time- and dose-dependent manner. 2-ME treatment resulted in an increased number of MG63 cells in the G_0/G_1 phase. Using an established nude mouse xenograft model *in vitro*, different concentrations of 2-ME inhibited tumor growth compared with the control group, and there was a dose-dependent association with 2-ME. The H&E staining results of nude mice xenografts demonstrated that the experimental groups exhibited different degrees of tumor cell density reduction and scattered tissue structure, with some cells exhibiting nuclear pyknosis and nuclear lysis. Collectively, these results demonstrate that 2-ME inhibited MG63 OS cell proliferation and xenograft growth.

2-ME induced both endogenous and exogenous apoptotic pathways in the present study, this may explain the broad-spectrum activity of 2-ME and the effects of 2-ME on a variety of cellular processes, including microtubule destruction, initiation of signal transduction pathways and production of reactive oxygen species, ultimately inducing apoptosis (37). Flow cytometry and TUNEL staining were used in the present study to detect apoptosis of tumor cells and xenograft tumor tissues, respectively. The results of the present study demonstrated that 2-ME induced apoptosis of MG63 cells and xenograft tumor cells in a dose-dependent manner.

In the present study. western blotting and RT-qPCR demonstrated that with increased 2-ME doses, the expression of caspase-3 in MG63 OS cells gradually increased and the expression of Bcl-2 and VEGF gradually decreased, suggesting that the expression of the aforementioned proteins depended on the dose of 2-ME. Immunohistochemical staining of nude mice xenografts demonstrated that with increased 2-ME concentrations, the expression of caspase-3 in tumor tissues gradually increased, and the expression of Bcl-2 and VEGF gradually decreased. In addition, apoptosis detected by TUNEL staining of xenograft tumors demonstrated that 2-ME induced apoptosis of MG63 OS cells and transplanted tumor tissues. The mechanism of apoptosis may be associated with Bcl-2 and caspase-3.

In contrast with other chemotherapeutic drugs, 2-ME has no issues with toxicity, such as gastrointestinal discomfort, hair loss and leukopenia (38). Even if the effective therapeutic dose of 2-ME is increased 12-fold, there has been no report of death due to treatment, only temporary weight loss and reversible changes in liver function, but no pathological changes (39). As 2-ME is loosely bound to estrogen, it does not have the carcinogenic risk of estrogen (40). In the present study, measurements of liver and kidney functional indicators revealed that 2-ME did not impair the liver and renal function of tumor-bearing nude mice suggesting that the anticancer activity of 2-ME has no short-term side effects.

A recent study has demonstrated that oleuropein alone or in combination with 2-ME, has anticancer effects on highly metastatic 143B OS cells and induces tumor cell autophagy (41). Notably, a synergistic effect between oleuropein and 2-ME on 143B OS cells was detected (41).

In summary, 2-ME had a strong inhibitory effect on OS both *in vitro* and *in vivo*. The mechanism by which 2-ME exerts its side effects may be associated with VEGF, Bcl-2 and caspase-3 with little or no side effects, which is of clinical significance for the treatment of patients with OS. To the best of our knowledge, no clinical trials on the treatment of OS with 2-ME have yet been conducted; therefore, further studies are warranted.

Acknowledgements

Not applicable.

Funding

No funding was received.

Availability of data and materials

The datasets used and/or analyzed during the present study is available from the corresponding author on reasonable request.

Authors' contributions

HT conceived and analyzed the experiments, HT, WX, LJ and XT performed the experiments and analysis. YZ analyzed the experimental data. HT wrote the manuscript and reviewed it for intellectual content. FT was involved in drafting the manuscript and revising it critically for important intellectual content, made substantial contributions to conception and design and acquisition of data, gave final approval of the version to be published and agreed to be accountable for all aspects of the work in ensuring that questions related to the accuracy or integrity of any part of the work are appropriately investigated and resolved. All authors have read and approved the manuscript.

Ethics approval and consent to participate

The animal experiments performed were approved by the Experimental Animal Care Committee (approval no. S01315022I) of Renmin Hospital, Wuhan University (Wuhan, China).

Patient consent for publication

Not applicable.

Competing interests

The authors declare that they have no competing interests.

References

1. Miwa S, Shirai T, Yamamoto N, Hayashi K, Takeuchi A, Igarashi K and Tsuchiya H: Current and emerging targets in immunotherapy for osteosarcoma. J Oncol 2019: 7035045, 2019.

2. Zhang Y, Yang J, Zhao N, Wang C, Kamar S, Zhou Y, He Z, Yang J, Sun B, Shi X, *et al*: Progress in the chemotherapeutic treatment of osteosarcoma. Oncol Lett 16: 6228-6237, 2018.
3. Teter Z, Śliwczyński A, Brzozowska M, Świerkowski M, Jacyna A, Pinkas J, Sierocka A, Marczak M, Dańska-Bidzińska A, Bidziński M and Wierzba W: The assessment of overall survival (OS) after adjuvant chemotherapy for patients with malignant endometrial cancer in Poland. Ginekol Pol 88: 296-301, 2017.
4. Wang C, Ren M, Zhao X, Wang A and Wang J: Emerging roles of circular RNAs in osteosarcoma. Med Sci Monit 24: 7043-7050, 2018.
5. Zou X, Zhou L, Zhu W, Mao Y and Chen L: Effectiveness of 2-methoxyestradiol in alleviating angiogenesis induced by intracranial venous hypertension. J Neurosurg 125: 746-753, 2016.
6. Zhang MZ, Liu YF, Ding N, Zhao PX, Zhang X, Liu MY, Adzavon YM, Huang JN, Long X, Wang XJ, *et al*: 2-Methoxyestradiol improves the apoptosis level in keloid fibroblasts through caspase-dependent mechanisms in vitro. Am J Transl Res 10: 4017-4029, 2018.
7. Dikshit A, Hales K and Hales DB: Whole flaxseed diet alters estrogen metabolism to promote 2-methoxtestradiol-induced apoptosis in hen ovarian cancer. J Nutr Biochem 42: 117-125, 2017.
8. Song LM, Wang GD, Wang HP and Xing NZ: Effect of 2-methoxyestradiol combined with quercetin on prostate cancer in vitro. Zhonghua Yi Xue Za Zhi 96: 95-99, 2016 (In Chinese).
9. Shi X, Wang Z, Xu F, Lu X, Yao H, Wu D, Sun S, Nie R, Gao S, Li P, *et al*: Design, synthesis and antiproliferative effect of 17β-amide derivatives of 2-methoxyestradiol and their studies on pharmacokinetics. Steroids 128: 6-14, 2017.
10. Kang SH, Cho HT, Devi S, Zhang Z, Escuin D, Liang Z, Mao H, Brat DJ, Olson JJ, Simons JW, *et al*: Antitumor effect of 2-methoxyestradiol in a rat orthotopic brain tumor model. Cancer Res 66: 11991-11997, 2006.
11. Nolte EM, Joubert AM, Lakier R, van Rensburg A and Mercier AE: Exposure of breast and lung cancer cells to a novel estrone analog prior to radiation enhances Bcl-2-mediated cell death. Int J Mol Sci 19: 2887, 2018.
12. Smolle MA, Leithner A, Posch F, Szkandera J, Liegl-Atzwanger B and Pichler M: MicroRNAs in different histologies of soft tissue sarcoma: A comprehensive review. Int J Mol Sci 18: 1960, 2017.
13. Zhao ZW, Yang LL, Ji JS, Zheng LY, Fang SJ and Wang JL: Effects and mechanism ofitraconazole on prostate cancer PC-3 cell apoptosis. Zhonghua Yi Xue Za Zhi 96: 3160-3163, 2016 (In Chinese).
14. Sun J, Zhang X, Sun Y, Tang ZS and Guo DY: Effects of hylomecon vernalis ethanol extracts on cell cycle and apoptosis of colon cancer cells. Mol Med Rep 15: 3485-3492, 2017.
15. Lee J, Jung MK, Park HJ, Kim KE and Cho D: Erdrl suppresses murine melanoma growth via regulation of apoptosis. Int J Mol Sci 17: 107, 2016.
16. van Vuuren RJ, Botes M, Jurgens T, Joubert AM and van den Bout I: Novel sulphamoylated 2-methoxy estradiol derivatives inhibit breast cancer migration by disrupting microtubule turnover and organization. Cancer Cell Int 19: 1, 2019.
17. Maran A, Zhang M, Kennedy AM, Sibonga JD, Rickard DJ, Spelsberg TC and Turner RT: 2-methoxyestradiol induces interferon gene expression and apoptosis in osteosarcoma cells. Bone 30: 393-398, 2002.
18. Guo X, Chen C, Liu X, Hou P, Guo X, Ding F, Wang Z, Hu Y, Li Z and Zhang Z: High oral bioavailability of 2-methoxyestradiol in PEG-PLGA micelles-microspheres for cancer therapy. Eur J Pharm Biopharm 117: 116-122, 2017.
19. Zhu J, Zhang W, Zhang Y, Wang Y, Liu M and Liu Y: Effects of Spica prunellae on caspase-3-associated proliferation and apoptosis in human lung cancer cells in vitro. J Cancer Res Ther 14: 760-763, 2018.
20. Nan Y, Wang S and Jia W: Caspase independent cleavages of TDP-43 generates 35 kD fragment that cause apoptosis of breast cancer cells. Biochem Biophys Res Commun 497: 51-57, 2018.
21. Grunewald S, Fitzl G and Springsguth C: Induction of ultra-morphological features of apoptosis in mature and immature sperm. Asian J Androl 19: 533-537, 2017.
22. Choudhary GS, Al-Harbi S and Almasan A: Caspase-3 activation is a critical determinant of genotoxic stress-induced apoptosis. Methods Mol Biol 1219: 1-9, 2015.
23. Treffkorn S and Mayer G: Conserved versus derived patterns of controlled cell death during the embryonic development of two species of Onychophora (velvet worms). Dev Dyn 246: 403-416, 2017.
24. Rogers C, Fernandes-Alnemri T, Mayes L, Alnemri D, Cingolani G and Alnemri ES: Cleavage of DFNA5 by caspase-3 during apoptosis mediates progression to secondary necrotic/pyroptotic cell death. Nat Commun 8: 14128, 2017.
25. Cianciulli A, Porro C, Calvello R, Trotta T and Panaro MA: Resistance to apoptosis in Leishmania infantum-infected human macrophages: A critical role for anti-apoptotic Bcl-2 protein and cellular IAP1/2. Clin Exp Med 18: 251-261, 2018.
26. Masuda H, Hirose J, Omata Y, Tokuyama N, Yasui T, Kadono Y, Miyazaki T and Tanaka S: Anti-apoptotic Bcl-2 family member Mcl-1 regulates cell viability and bone-resorbing activity of osteoclasts. Bone 58: 1-10, 2014.
27. Villanova L, Careccia S, De Maria R and Fiori ME: Micro-economics of apoptosis in cancer: NcRNAs modulation of BCL-2 family members. Int J Mol Sci 19: 958, 2018.
28. Alzate JM, Montoya-Florez LM, Pérez JE, Rocha NS and Pedraza-Ordonez FJ: The role of the multi-drug resistance 1, p53, b cell lymphoma 2, and BCL 2-associated X genes in the biologic behavior and chemotherapeutic resistance of canine transmissible venereal tumors. Vet Clin Pathol 48: 730-739, 2019.
29. Ebrahim AS, Sabbagh H, Liddane A, Raufi A, Kandouz M and Al-Katib A: Hematologic malignancies: Newer strategies to counter the BCL-2 protein. J Cancer Res Clin Oncol 142: 2013-2022, 2016.
30. Qiu XG, Chen YD, Yuan J, Zhang N, Lei T, Liu J and Yang M: Functional BCL-2 rs2279115 promoter noncoding variant contributes to glioma predisposition, especially in males. DNA Cell Biol 38: 85-90, 2019.
31. Ghasemi A, Khanzadeh T, di Heydarabad M, Khorrami A, Jahanban Esfahlan A, Ghavipanjeh S, Gholipour Belverdi M, Darvishani Fikouhi S, Darbin A, Najafpour M and Azimi A: Evaluation of BAX and BCL-2 gene expression and apoptosis induction in acute lymphoblastic leukemia cell line CCRFCEM after High- dose prednisolone treatment. Asian Pac J Cancer Prev 19: 2319-2323, 2018.
32. Bui NL, Pandey V, Zhu T, Ma L, Basappa and Lobie PE: Bad phosphorylation as a target of inhibition in oncology. Cancer Lett 415: 177-186, 2018.
33. Wu Y, Zhao D, Zhuang J, Zhang F and Xu C: Caspase-8 and caspase-9 functioned differently at different stages of the cyclic stretch-induced apoptosis in human periodontal ligament cells. PLoS One 11: e0168268, 2016.
34. Livak KJ and Schmittgen TD: Analysis of relative gene expression data using real-time quantitative PCR and the 2(-Delta Delta C(T)) method. Methods 25: 402-408, 2001.
35. Watts FM Jr, Pouland T, Bunce RA, Berlin KD, Benbrook DM, Mashayekhi M, Bhandari D and Zhou D: Activity of oxygen-versus sulfur-containing analogs of the Flex-Het anticancer agent SHetA2. Eur J Med Chem 158: 720-732, 2018.
36. Yao L, Zou X, Jin C, Fan J, Guo Z, Lin Q, Li J and Fu D: The roles of ID-1 in human pancreatic ductal adenocarcinoma and the therapeutic effects of 2-methoxyestradiol. Carcinogenesis 39: 728-737, 2018.
37. Minorics R and Zupko I: Steroidal anticancer agents: An overview of estradiol-related compounds. Anticancer Agents Med Chem 18: 652-666, 2018.
38. Lundström-Stadelmann B, Rufener R, Ritler D, Zurbriggen R and Hemphill A: The importance of being parasiticidal an update on drug development for the treatment of alveolar echinococcosis. Food Waterborne Parasitol 15: e00040, 2019.
39. Shen Z, Wu Y, Chen X, Chang X, Zhou Q, Zhou J, Ying H, Zheng J, Duan T and Wang K: Decreased maternal serum 2-methoxyestradiol levels are associated with the development of preeclampsia. Cell Physiol Biochem 34: 2189-2199, 2014.
40. Caporarello N, Lupo G, Olivieri M, Cristaldi M, Cambria MT, Salmeri M and Anfuso CD: Classical VEGF, Notch and ang signalling in cancer angiogenesis, alternative approaches and future directions (Review). Mol Med Rep 16: 4393-4402, 2017.
41. Przychodzen P, Wyszkowska R, Gorzynik-Debicka M, Kostrzewa T, Kuban-Jankowska A and Gorska-Ponikowska M: Anticancer potential of oleuropein, the polyphenol of olive oil, with 2-methoxyestradiol, separately or in combination, in human osteosarcoma cells. Anticancer Res 39: 1243-1251, 2019.